Journal of Clinical and Translational Hepatology **2024**
DOI: 10.14218/JCTH.2024.00233

Original Article

ADAMTS13 Improves Hepatic Platelet Accumulation in Pyrrolizidine Alkaloids-induced Liver Injury

Mingyan Ji[1,2#], Yun Chen[1,2#], Yifan Ma[1,2], Dongping Li[1,2], Jin Ren[3], Hongyue Jiang[1,2], Sinuo Chen[1,2], Xiaoqing Zeng[1,2*] and Hong Gao[1,2,4*]

[1]Department of Gastroenterology and Hepatology, Zhongshan Hospital, Fudan University, Shanghai, China; [2]Shanghai Institute of Liver Disease, Shanghai, China; [3]Guizhou University School of Medicine, Guiyang, Guizhou, China; [4]Center for Evidence-Based Medicine, Fudan University, Shanghai, China

Received: July 15, 2024 | **Revised:** October 12, 2024 | **Accepted:** November 01, 2024 | **Published online:** November 22, 2024

Abstract

Background and Aims: Pyrrolizidine alkaloids (PAs), widely distributed in plants, are known to induce liver failure. Hepatic platelet accumulation has been reported during the progression of PA-induced liver injury (PA-ILI). This study aimed to investigate the mechanisms underlying platelet accumulation in PA-ILI. ***Methods:*** Cases of PA-ILI, non-PA-ILI, and control subjects were collected from patients hospitalized at Zhongshan Hospital, Fudan University (Shanghai, China) between 2012 and 2019. A mouse model of PA-ILI was established using monocrotaline administration. Liver RNA sequencing was performed, and gene interactions were analyzed using the Search Tool for the Retrieval of Interacting Genes/Proteins online database. Low-molecular-weight heparin and recombinant a disintegrin and metalloproteinase with a thrombospondin type I motif member 13 (ADAMTS13) were applied. The necrotic liver area, hepatic platelet accumulation, and von Willebrand factor (VWF) deposition were examined using hematoxylin and eosin staining and immunofluorescence assay. ***Results:*** Hepatic platelet accumulation, necrotic area expansion, and increased VWF expression were observed in both PA-ILI patients and mice. The Search Tool for the Retrieval of Interacting Genes/Proteins database indicated that ADAMTS13 regulates VWF expression and was differentially expressed in the livers of PA-ILI mice. Plasma and hepatic ADAMTS13 levels were significantly downregulated in both PA-ILI patients and mice. Systemic administration of recombinant ADAMTS13 decreased hepatic platelet accumulation, downregulated VWF expression, and mitigated mouse hepatic necrosis. ***Conclusions:*** Hepatic platelet accumulation in PA-ILI was confirmed in both patients and mice. Deficiency of ADAMTS13 plays a critical role in platelet accumulation in PA-ILI, suggesting that ADAMTS13 could be a potential therapeutic target for this condition.

Citation of this article: Ji M, Chen Y, Ma Y, Li D, Ren J, Jiang H, *et al*. ADAMTS13 Improves Hepatic Platelet Accumulation in Pyrrolizidine Alkaloids-induced Liver Injury. J Clin Transl Hepatol 2024. doi: 10.14218/JCTH.2024.00233.

Keywords: Pyrrolizidine alkaloids; Liver injury; PA-ILI; Platelet accumulation; ADAMTS13; von Willebrand factor; VWF.

[#]Contributed equally to this work.
[*]**Correspondence to:** Hong Gao and Xiaoqing Zeng, Department of Gastroenterology and Hepatology, Zhongshan Hospital, Fudan University, No. 180 Fenglin Road, Xuhui District, Shanghai 200032, China. ORCID: https://orcid.org/0000-0002-2263-9214 (HG) and https://orcid.org/0000-0003-3494-8636 (XZ). Tel +86-13611673691, Fax +86-21-64432583, E-mail gao.hong@zs-hospital.sh.cn (HG) and zeng.xiaoqing@zs-hospital.sh.cn (XZ).

Introduction

Herbs and their components account for 25.3% of drug-induced liver injuries,[1] with a higher prevalence observed in Eastern countries. Pyrrolizidine alkaloids (PAs)-induced hepatotoxicity is an increasing concern in clinical practice,[2] due to the detection of PAs in common dietary items.[3] Pyrrolizidine alkaloids-induced liver injury (PA-ILI) is characterized by hepatic sinusoidal obstruction, which can be partly attributed to platelet aggregation.[4,5] Importantly, PA-ILI patients present with a reduced count of peripheral platelets,[6] indicating systemic hematological changes during the progression of PA-ILI that resemble the pathological conditions seen in acute liver failure.[7]

Von Willebrand factor (VWF) plays a crucial role in regulating platelet accumulation and clearance.[8] Blocking VWF reduces hepatic platelet accumulation and promotes liver repair in cases of acetaminophen-induced liver injury.[8] The presence of VWF is regulated by metalloproteinases, particularly a disintegrin and metalloproteinase with a thrombospondin type I motif member 13 (ADAMTS13).[9] Studies have shown that an increased VWF/ADAMTS13 ratio may correlate with poor outcomes in patients with acute liver injury[10] and hepatic carcinoma.[11] This suggests that alterations in the VWF/ADAMTS13 ratio could regulate hepatic platelet activity in PA-ILI. Therefore, this study investigated the roles of ADAMTS13 and VWF in PA-ILI in both mice and patients, focusing specifically on platelet accumulation in the liver.

Methods

Establishment of a mouse model

Experiments were conducted on eight-week-old mice (male, C57BL/6J mice, Beijing Vital River Laboratory, Beijing, China) selected randomly. All procedures involving animals complied with the Guide for the Care and Use of Laboratory Animals (8th edition, revised 2011) by the US National

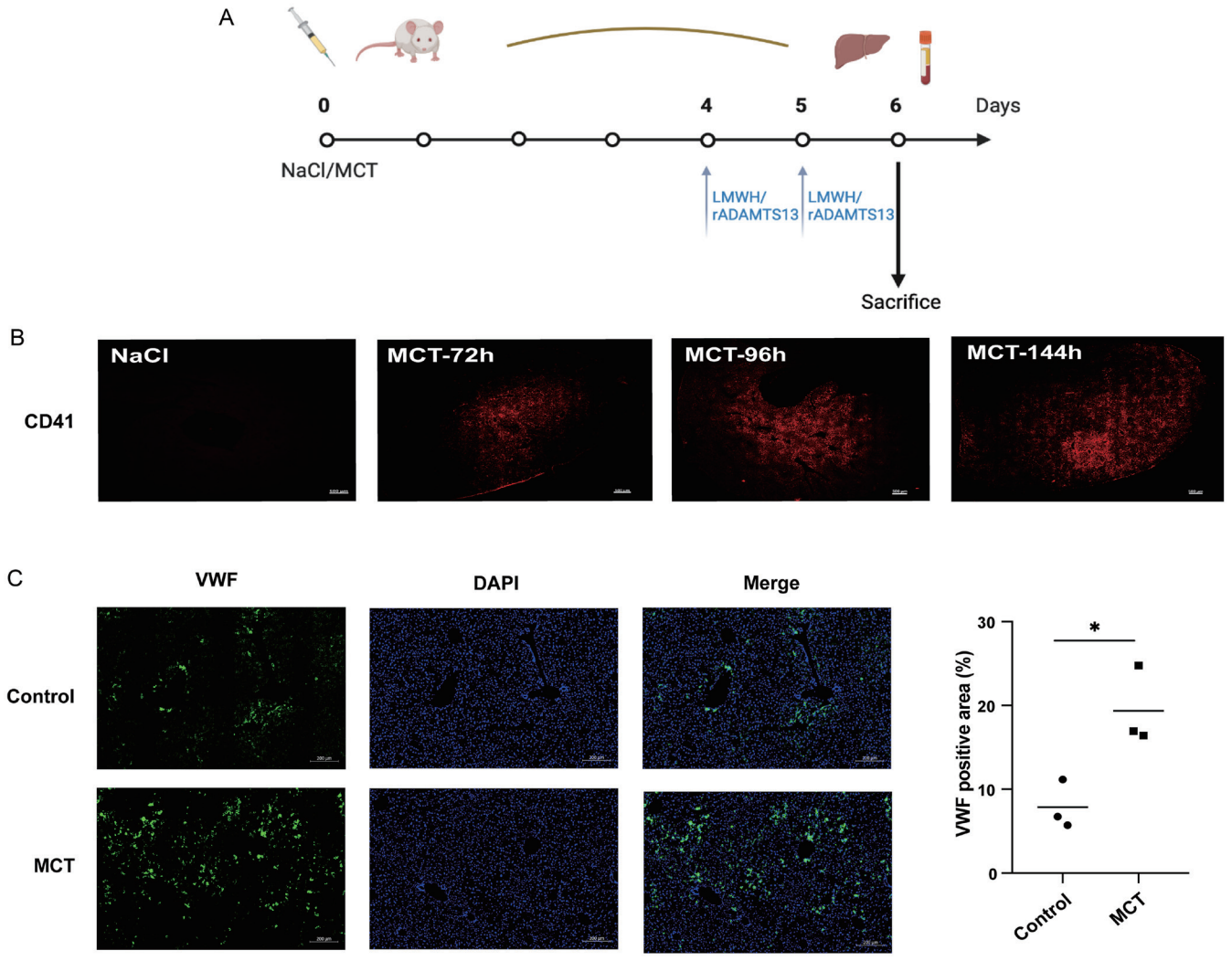

Fig. 1. Hepatic platelet accumulation and VWF distribution in PA-ILI mice. (A) Animal setting and treatments in mice with PA-ILI. (B) Representative images of hepatic platelets (red) in PA-ILI mice (n = 3). (C) Representative images (left) and quantification (right) of VWF (green) in PA-ILI mice (n = 3). *$p < 0.05$. VWF, von Willebrand factor; PA-ILI, pyrrolizidine alkaloids-induced liver injury; LMWH, low-molecular-weight heparin; DAPI, 4',6-diamidino-2-phenylindole; MCT, monocrotaline.

Institutes of Health and were approved by the Animal Care and Use Committee of Zhongshan Hospital, Fudan University (Shanghai, China; Approval No. 2020-006).

To induce PA-ILI, monocrotaline (MCT; C101556, 400 mg/kg; Aladdin, Shanghai, China), a toxic PA, was administered via intragastric gavage for six days. A 0.9% sodium chloride solution served as the solvent control.[12] To assess platelet accumulation's involvement in PA-ILI, Fraxiparine (0.1 mL/10 kg), a low-molecular-weight heparin (LMWH), was administered subcutaneously on day (D) 4 and D5. The role of ADAMTS13 was evaluated by injecting recombinant ADAMTS13 (1 μg dissolved in 100 μL endotoxin-free PBS) via the tail vein on D4 and D5 (Fig. 1A). Liver and blood samples were collected for analysis.

Patients and samples

Demographic and laboratory data from confirmed drug-induced liver injury cases, hospitalized from 2012 to 2019 at Zhongshan Hospital, Fudan University, were collected.

To diagnose PA-ILI, the Nanjing criteria were applied in this study.[13] Non-PA-ILI patients were also included (i.e., those with a history of taking medications not containing PAs within the past three months and a Roussel Uclaf Causality Assessment Method score greater than three). Patients diagnosed with viral infections, autoimmune diseases, alcohol abuse, fatty liver, heart failure, Budd-Chiari syndrome, congenital liver disease, or liver carcinoma were excluded from both the PA-ILI and non-PA-ILI groups. Patients lacking information on their medications were also excluded.[14] The 5-point scale from the Drug-Induced Liver Injury Network (DILIN) was used to assess the severity of liver injury.

Cancer-adjacent normal tissue samples from patients with liver malignancies served as the control group. Hematoxylin and eosin staining of these liver tissues showed no signs of congestion, sinusoidal dilation, or inflammatory response, and liver cell structures appeared neatly arranged. Liver biopsy samples from PA-ILI and non-PA-ILI cases, as well as adjacent non-tumor liver tissues from hepatic cancer patients (control group), were collected [Zhongshan Hospital, Fudan University, Approval No. B2018-070(2)]. Patient plasma samples were stored at −80°C for ADAMTS13 detection.

High-throughput RNA sequencing (RNA-seq) and bioinformatic analysis

High-throughput RNA-seq was conducted using the Tusanqi-induced liver injury model. Tusanqi is widely utilized in traditional Chinese medicine, but it may cause liver injury[15,16] due to its content of four PAs: senecionine, seneciphylline, seneciphylline N-oxide, and senecionine N-oxide. According to our previous study, Tusanqi-induced liver injury in mice was also applied in this study. FASTQ data were analyzed using fastp,[17] HISAT2,[18] and htseq-count[19] programs. Differentially expressed genes (DEGs) were identified using the "DEseq2" package in R,[20] when their fold change > 1 and adjusted *p*-value < 0.05. The "ClusterProfiler" package[21] was used to explore the biological processes of DEGs. The STRING online database (https://www.string-db.org/) was used to predict potential correlations between VWF and DEGs.[22] RNA-seq data were deposited in the Gene Expression Omnibus database (GSE171874).

Measurement of mouse liver injury

Alanine aminotransferase (ALT) and aspartate aminotransferase (AST) kits were obtained from Wuhan Servicebio Culture Consulting Co., Ltd. (Wuhan, China). Paraffin-embedded liver tissues underwent hematoxylin and eosin staining. To assess liver necrotic areas, at least two sections from the left lateral lobe of each mouse and patient sample were evaluated and quantified by a blinded technician using ImageJ software. Liver sections were scanned using the Zeiss Scan Z1 system (Carl Zeiss AG, Oberkochen, Germany).

Immunofluorescence staining

Fibrinogen, ADAMTS13, VWF, and CD41 were detected by immunofluorescence staining. Antigen retrieval was conducted at 100°C for 15 m in Tris-EDTA (pH 9.0). After blocking with 10% normal goat serum at room temperature for 1 h, antibodies against CD41 (ab134131, 1:50 for mouse samples and 1:200 for human samples; Abcam, Cambridge, UK), VWF (ab11713, 1:200; Abcam), and fibrinogen gamma (FGG; 15841-1-AP, 1:100; Proteintech, Wuhan, China) were incubated at 4°C overnight. Corresponding secondary antibodies were applied the following day. Fluorescence images were obtained using the Zeiss Scan Z1 system and analyzed with ImageJ software. Positive areas of platelet accumulation and VWF were quantified in three to four randomly selected images per sample.

ELISA

Plasma ADAMTS13 levels were measured using a Human ADAMTS13 Quantikine ELISA kit (DADT130; R&D Systems, Minneapolis, MN, USA) per the manufacturer's instructions.[23]

RNA extraction and real-time PCR analysis

Total RNA was extracted from mouse liver tissues using a Total RNA Kit (DP419; Tiangen, Beijing, China) and synthesized into cDNA using the Superscript II reverse transcriptase kit (TOYOBO, Tokyo, Japan). Quantitative PCR amplification was conducted using a Roche LightCycler® 480 II Real-time PCR system and SYBR Green (Tiangen). Primer sequences for GAPDH and ADAMTS13 are presented in Supplementary Table 1.

Western blot analysis

Protein concentrations of cell and tissue lysates were determined using a BCA protein assay kit (Beyotime, Shanghai, China). Proteins were separated via sodium dodecyl sulfate-polyacrylamide gel electrophoresis, and primary antibodies were used to detect caspase-3 (9665S, 1:1,000; Cell Signaling Technology, Danvers, MA, USA), cleaved caspase-3 (9661T, 1:1,000; Cell Signaling Technology), FGG (15841-1-AP, 1:1,000; Proteintech), ADAMTS13 (A8482, 1:1,000; ABclonal, Woburn, MA, USA), and β-actin (1:5,000; Sigma-Aldrich, St. Louis, MO, USA). Protein expression was quantified using ImageJ software.

Statistical analysis

Data were analyzed using GraphPad Prism 9.0 software (GraphPad Software Inc., La Jolla, CA, USA). Student's t-test was applied to determine statistical significance, with data presented as mean ± standard deviation. A *p*-value < 0.05 was considered statistically significant.

Results

Hepatic platelet accumulation and increased VWF expression were observed in PA-ILI mice and patients

Apparent hepatocyte death and congestion were noted in mouse livers stimulated with MCT (Supplementary Fig. 1). The TUNEL assay showed increased apoptotic areas in MCT-induced mice (Supplementary Fig. 1). Accumulation of platelets, as indicated by CD41 staining (also known as platelet glycoprotein [GP] IIb/IIIa), was found in the MCT-stimulated livers but not in the control mice (Fig. 1B). Given that VWF regulates platelet adhesion and accumulation through GPIb/V/IX and CD41,[24] further experiments demonstrated that VWF expression was upregulated in the MCT-induced mouse model (Fig. 1C).

In PA-ILI patients, pathological examination revealed hepatic sinus dilatation and congestion in the liver (Supplementary Fig. 2A). CD41 expression was significantly elevated in PA-ILI patients compared to the control group ($p = 0.0004$) and non-PA-ILI patients ($p = 0.0006$) (Fig. 2A). Moreover, VWF protein expression was significantly increased in PA-ILI patients compared to non-PA-ILI patients ($p = 0.0105$) and the control group ($p = 0.0404$) (Fig. 2B).

Reduction in platelet accumulation with the improvement of hepatic function

LMWH, a traditional anticoagulant targeting factors IIa (thrombin) and Xa, has been reported to reduce platelet deposition.[25,26] In the present study, LMWH treatment significantly reduced CD41 expression in MCT-induced mice ($p = 0.0460$) (Fig. 3A). Furthermore, LMWH treatment reduced the hepatic necrotic area ($p = 0.0008$) (Fig. 3B) and significantly improved plasma ALT and AST levels in MCT-induced mice (ALT: MCT vs. MCT+LMWH, 350.2455 ± 284.5684 vs. 40.9105 ± 10.2209 U/L, $p = 0.0252$; AST: MCT vs. MCT+LMWH, 283.8675 ± 130.7658 vs. 78.0098 ± 13.8228 U/L, $p = 0.0204$).

These data indicate that hepatic platelet accumulation and VWF upregulation occurred in both PA-ILI mouse and patient groups. Preventing these changes led to reversals of these effects and improvement in function.

Activation of the coagulation cascade is one of the mechanisms leading to platelet aggregation.[27] However, in the present study, hepatic expression of FGG was unchanged in PA-ILI patients compared to both the control group and non-PA-ILI patients (Supplementary Fig. 2B), indicating that the coagulation cascade was not activated in PA-ILI patients.

Prediction of ADAMTS13 as a regulator of VWF in PA-ILI by bioinformatic analysis

RNA-seq identified 1,209 DEGs, with 631 upregulated and

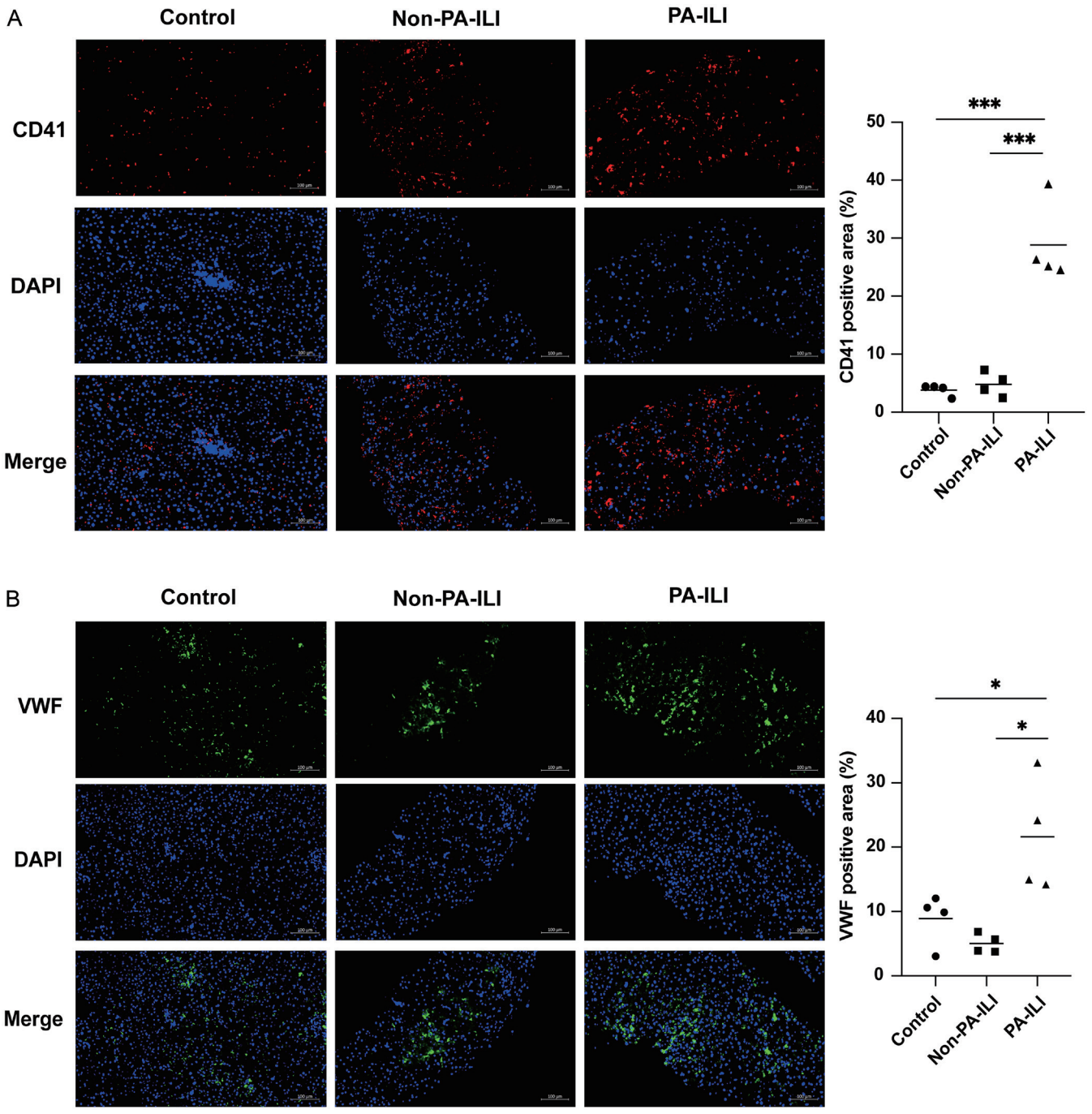

Fig. 2. Hepatic platelet accumulation and VWF distribution in PA-ILI patients. (A) Representative images (left) and quantification (right) of CD41 protein (red) in patients (n = 4). (B) Representative images (left) and quantification (right) of VWF protein (green) in patients (n = 4). *$p < 0.05$, ***$p < 0.001$. VWF, von Willebrand factor; PA-ILI, pyrrolizidine alkaloids-induced liver injury; DAPI, 4′,6-diamidino-2-phenylindole.

578 downregulated genes in the PA-ILI group compared to the control group (Fig. 4A and B). Biological processes related to wound healing, hemostasis, coagulation, and platelet-related pathways were enriched (Fig. 4C and D). To explore potential regulators of VWF and platelet accumulation, VWF-related proteins (Fig. 4E), sorted upstream and downstream by the STRING[22] were compared with DEGs associated with these biological processes. This analysis identified three genes: Selp (Selectin P), which was upregulated, and F8 (Coagulation Factor VIII) and ADAMTS13, which were both downregulated (Fig. 4F).

Reduced expression of ADAMTS13 protein regulates VWF upregulation in PA-ILI

F8, a stable coagulation factor, is activated by separating from the VWF molecule under pathological conditions.[28] Giv-

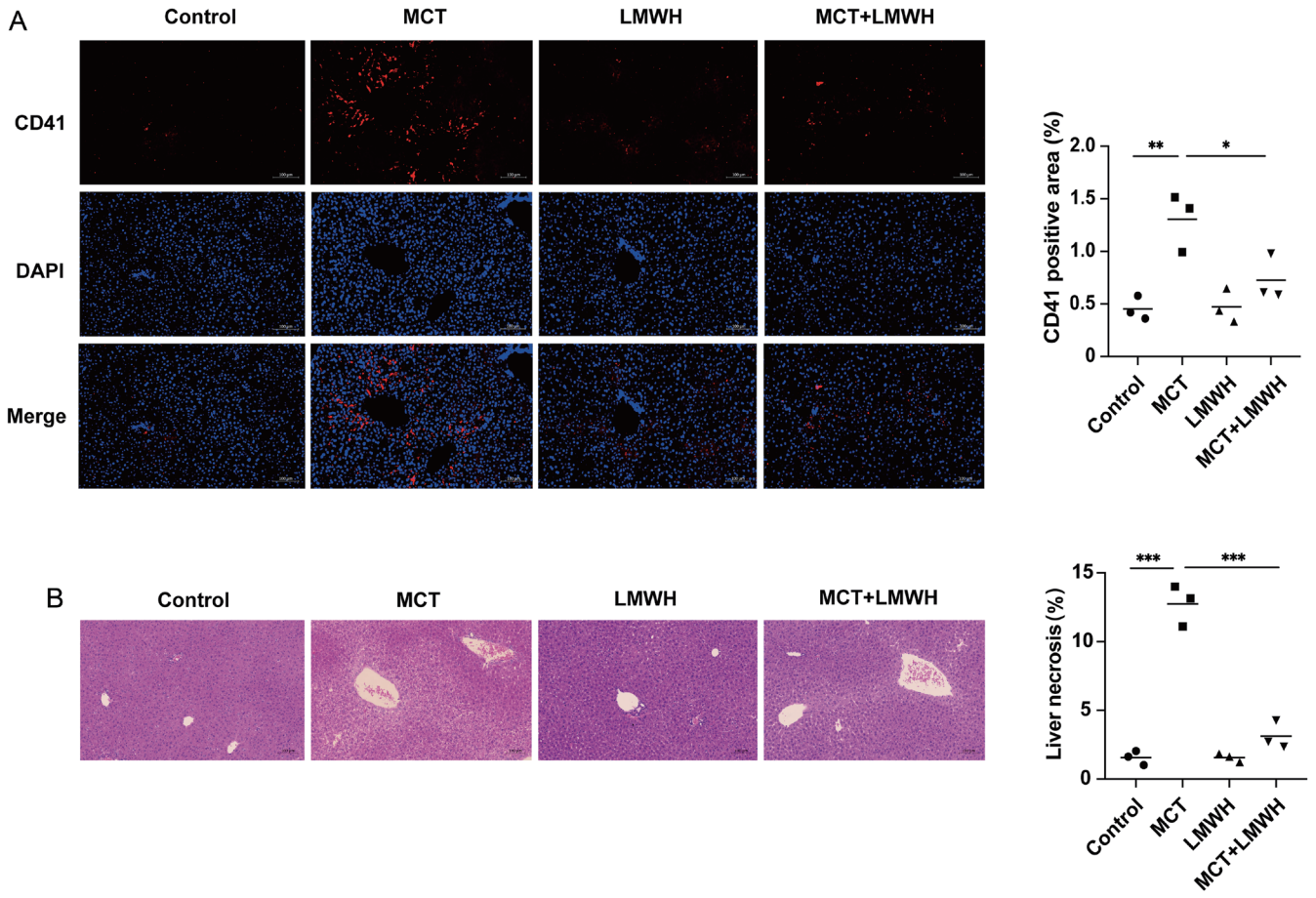

Fig. 3. LMWH treatment mitigates hepatic platelet accumulation. (A) Representative images (left) and quantification (right) of CD41 protein (red) in mice (n = 3). (B) Hematoxylin and eosin staining (left) of liver tissues, with quantification (right) of the hepatic necrosis area (n = 3). *p < 0.05, **p < 0.01, ***p < 0.001. LMWH, low-molecular-weight heparin; MCT, monocrotaline; DAPI, 4′,6-diamidino-2-phenylindole.

en that Selp protein was not detected in the liver, attention was directed toward ADAMTS13, a circulating metalloproteinase that modulates VWF activity.[29]

Hepatic ADAMTS13 levels were reduced in the PA-ILI group compared to the control group (p = 0.0310) and non-PA-ILI patients (p = 0.0228) (Fig. 5A). Plasma ADAMTS13 levels were also downregulated in the PA-ILI group compared to non-PA-ILI patients (p < 0.0001) (Fig. 5B). Furthermore, peripheral platelet count (p = 0.0120) and plasma ADAMTS13 levels (p = 0.0015) were significantly lower in cases of severe liver injury (grade 3-4) than in mild liver injury cases (grade 1-2) (Fig. 5B).

In the mouse model, plasma ADAMTS13 levels were decreased in the MCT group compared to the control group (Fig. 5C). Both mRNA (Fig. 5D) and protein (Fig. 5E and F) expression levels of ADAMTS13 in the liver were reduced, while an upregulation of ADAMTS13 protein was observed in kidney tissue, with no significant changes noted in lung tissue (Fig. 5C). Additionally, there was a gradual decrease in ADAMTS13 protein levels over time (72 h, 96 h, and 144 h) under MCT influence, while both cleaved and total caspase 3 protein levels were elevated (Fig. 5E).

Administration of rADAMTS13 significantly restored plasma levels and protein expression of ADAMTS13 in the liver of MCT mice (Fig. 6A), reduced liver necrotic area (Fig. 6B and C), and decreased CD41 (p = 0.0005) and VWF (p = 0.0223) protein expression levels (Fig. 6D). Liver abnormalities were evident, although blood abnormalities were not yet apparent, as shown in Supplementary Figure 3.

Discussion

The present study found that downregulation of ADAMTS13 led to increased platelet accumulation in the liver, which could be involved in the pathogenesis of PA-ILI. The severity of liver injury was related to both peripheral platelet count and ADAMTS13 deficiency. Preventing platelet accumulation with rADAMTS13 reduced cell necrosis and restored liver function.

The role of platelet accumulation in liver disease remains controversial.[30] Platelet aggregation promotes liver regeneration in liver transplantation patients,[31] yet it deteriorates liver function in patients with hepatocellular carcinoma,[32] nonalcoholic hepatitis,[32] and ischemia–reperfusion liver disease. Contrary to a previous study,[33] the present study revealed that alleviating hepatic platelet accumulation through LMWH or rADAMTS13 reduced PA-ILI, suggesting that platelet accumulation contributes to PA-ILI and leads to liver impairment.

ADAMTS13 cleaves VWF multimers by recognizing multiple A2 sites in the VWF domain. Recombinant ADAMTS13 has primarily been documented in the literature to exhibit no adverse effects on the liver.[34,35] In our investigation, the group treated exclusively with rADAMTS13 showed no significant

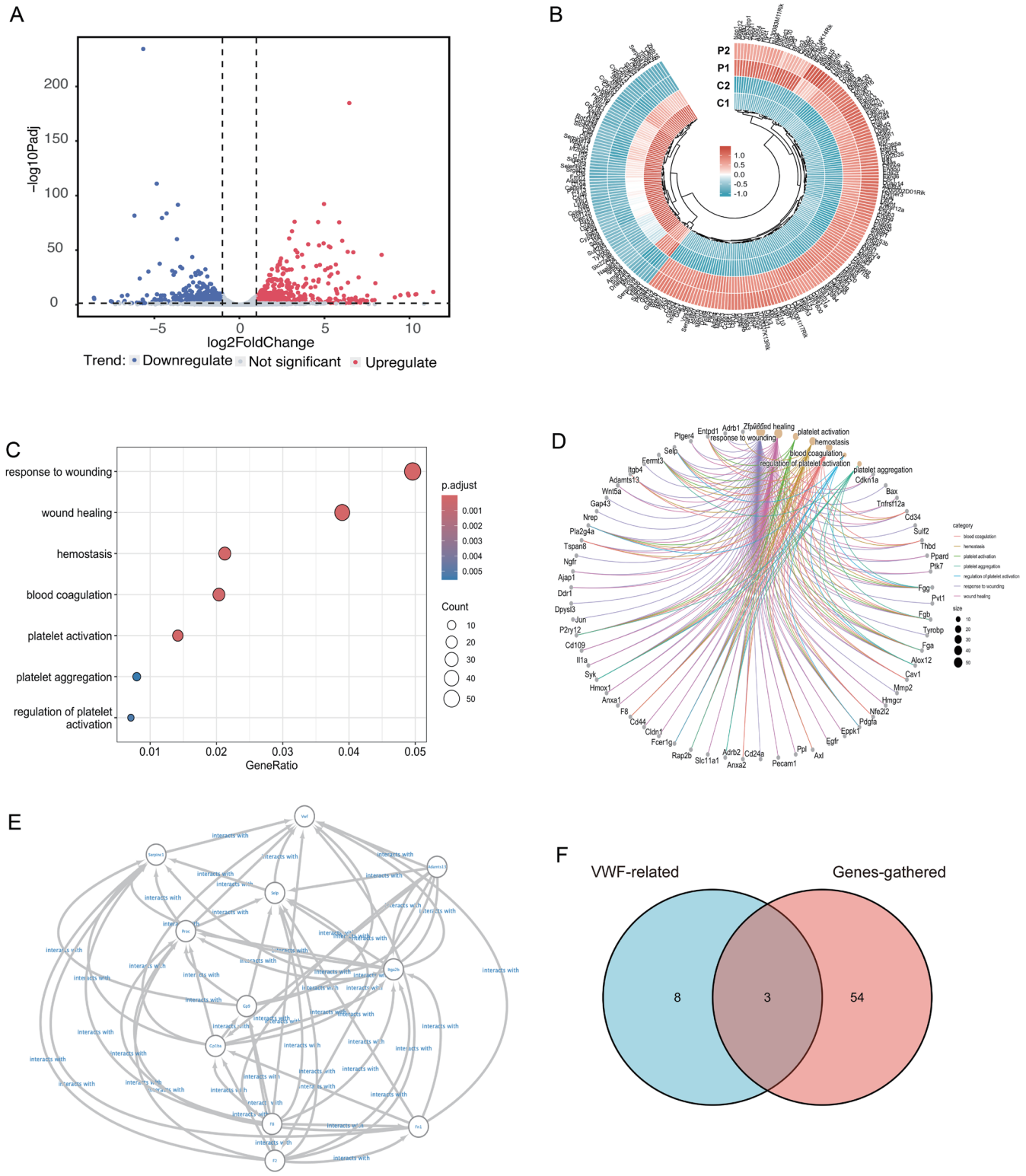

Fig. 4. RNA sequencing of the liver in PA-ILI mice. (A) Volcano plots of DEGs (PA-ILI group vs. control group). (B) Heatmap of the top 250 genes between PA-ILI mice (groups P1 & P2) and controls (groups C1 & C2). (C) Dot plots of seven GO biological process categories, including wound healing, hemostasis, coagulation, and platelet-related pathways. (D) Cnetplot displaying 57 DEGs assigned to the seven GO biological process categories. (E) Protein–protein interaction data of VWF from STRING, containing 11 nodes and 104 edges. (F) Venn diagram of 57 DEGs (red) and 11 VWF-related genes (blue) with three shared genes in the overlapping regions, including ADAMTS13. PA-ILI, pyrrolizidine alkaloids-induced liver injury; VWF, von Willebrand factor; DEG, differentially expressed genes; GO, Gene Ontology; STRING, Search Tool for the Retrieval of Interacting Genes/Proteins.

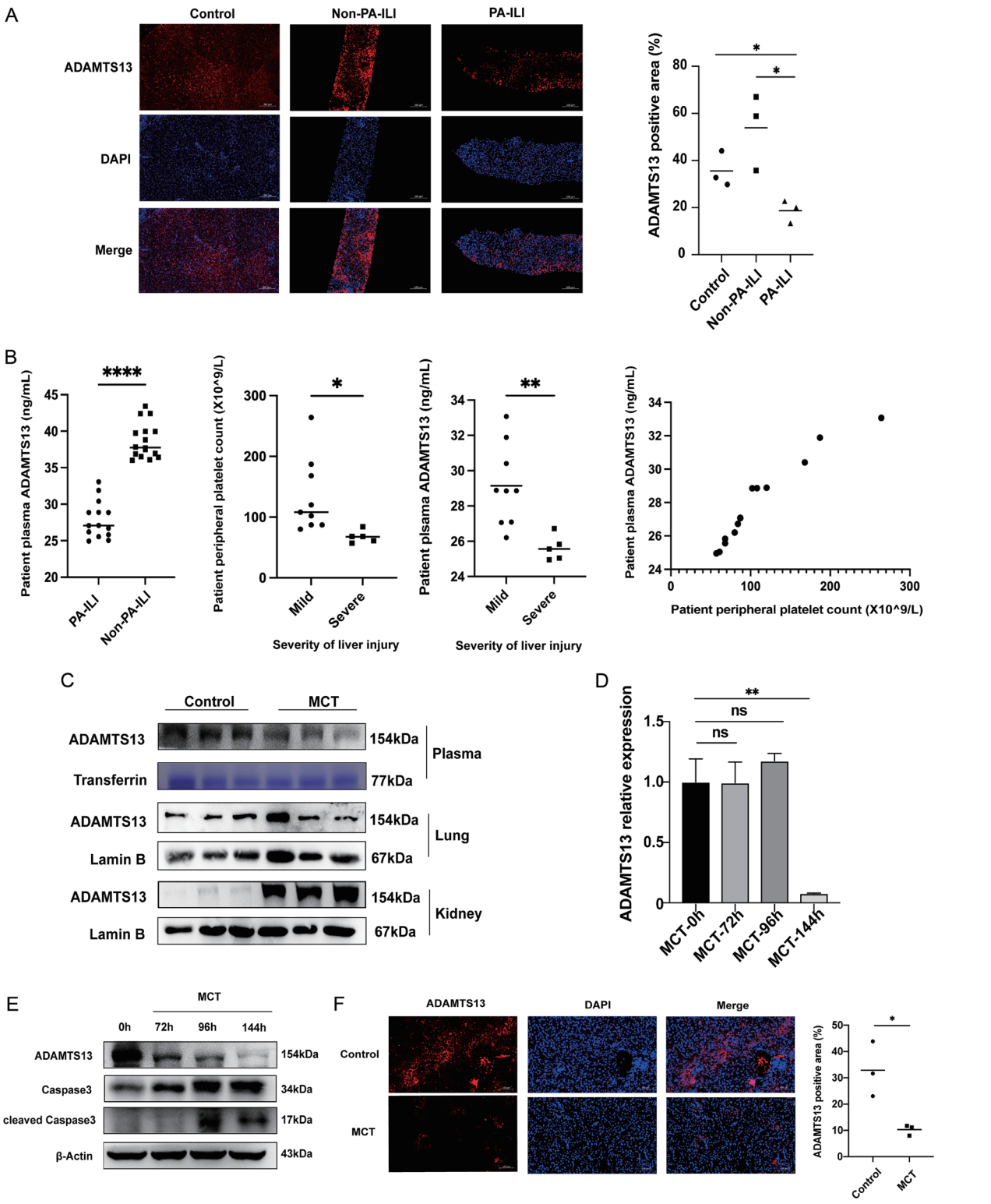

Fig. 5. Hepatic ADAMTS13 expression is reduced in PA-ILI. (A) Representative images (left) and quantification (right) of hepatic ADAMTS13 (red) in patients (n = 3). (B) Plasma level of ADAMTS13 in patients (leftmost). Peripheral platelet count and plasma ADAMTS13 concentration in mild and severe PA-ILI (middle). Relationship between peripheral platelet count and plasma ADAMTS13 in PA-ILI patients (rightmost). (C) Representative Western blots of ADAMTS13 in mouse plasma, lungs, and kidneys. (D) Hepatic mRNA level of ADAMTS13 in MCT-treated mice. (E) Representative Western blots of ADAMTS13 and apoptosis-related proteins. (F) Representative images (left) and quantification (right) of hepatic ADAMTS13 (red) in the mouse liver (n = 3). *$p < 0.05$, **$p < 0.01$, ****$p < 0.0001$. PA-ILI, pyrrolizidine alkaloids-induced liver injury; DAPI, 4′,6-diamidino-2-phenylindole; MCT, monocrotaline.

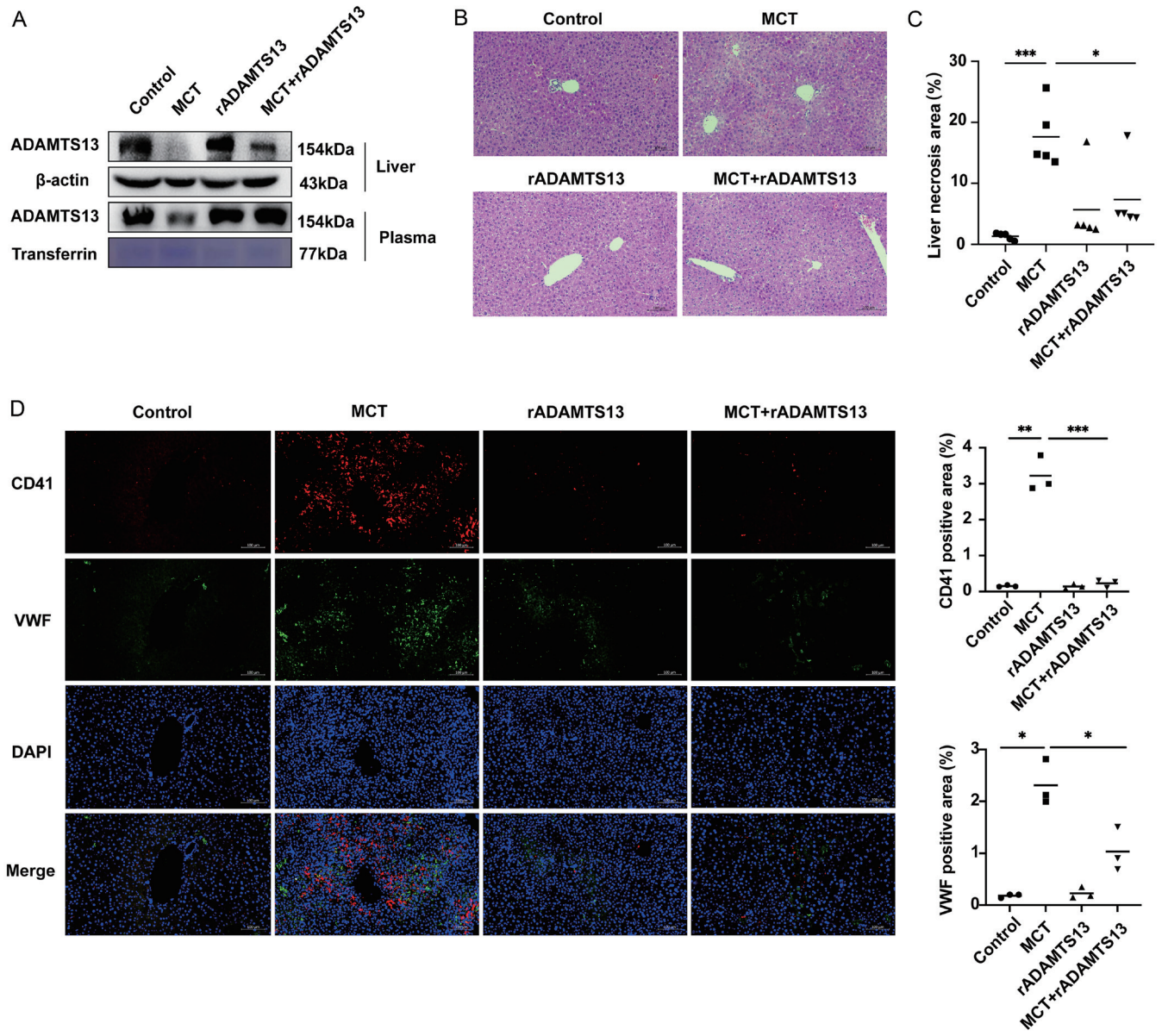

Fig. 6. ADAMTS13 treatment alleviates hepatic platelet accumulation. (A) Representative Western blots and quantification of plasma and hepatic ADAMTS13 protein. (B) Pathological changes in PA-ILI mice treated with rADAMTS13. (C) Measurement of hepatic necrosis (n = 5). (D) Representative images (left) and quantification (right) of hepatic platelets (CD41, red) and VWF deposition (green). *$p < 0.05$, **$p < 0.01$, ***$p < 0.001$. PA-ILI, pyrrolizidine alkaloids-induced liver injury; VWF, von Willebrand factor; DAPI, 4′,6-diamidino-2-phenylindole; MCT, monocrotaline.

differences in ALT levels compared to the control group, with both groups maintaining low values. Although the ALT level in the group treated with both MCT and rADAMTS13 was slightly lower than in the MCT-only group, this difference was not statistically significant, potentially due to the prolonged half-life of ALT, which can extend up to 57 h (Supplementary Fig. 3). The downregulation of ADAMTS13 in both patients and the mouse model contributed to increased hepatic VWF protein expression and platelet accumulation in PA-ILI. Recombinant ADAMTS13 was able to reduce hepatic platelet accumulation and alleviate PA-ILI.

According to findings by Masahito Uemura *et al*.[36] and Nancy A. Turner *et al*.,[37] hepatic stellate cells may be the primary cellular source of ADAMTS13 in the human liver. Additionally, ADAMTS13 has been detected in vascular endothelial cells and human platelets.[37] However, these results do not specifically address drug-induced liver injury. The precise origin of ADAMTS13 in liver injury associated with PA-ILI remains uncertain. We measured ADAMTS13 protein expression in cultured hepatic, stellate, and endothelial cells stimulated with MCT. After 24 h of stimulation, MCT significantly reduced ADAMTS13 expression in cultured hepatic cells, but not in stellate or endothelial cells (Supplementary Fig. 4). Based on these preliminary findings, hepatocytes may act as the principal source of ADAMTS13 in this disease context. Therefore, in PA-ILI, impaired hepatocytes produce less ADAMTS13, leading to increased VWF expression and platelet aggregation in a vicious cycle. Further validation of these

findings will require additional investigations using primary cell cultures or other model systems.

Conclusions

Hepatic platelet accumulation plays a significant role in PA-ILI, and reduced ADAMTS13 protein expression leads to increased hepatic VWF expression and further platelet accumulation. Targeting ADAMTS13 may represent a promising approach for PA-ILI treatment, warranting further investigation.

Acknowledgments

We thank Professor Ronggui Hu (Institute of Biochemistry and Cell Biology, Shanghai Institutes for Biological Sciences, Chinese Academy of Sciences) for research guidance and technical support. We also thank Ms. Hua (Selin) He from Medjaden Inc. (www.medjaden.com) and Professor Yi Shi (Zhongshan Hospital, Fudan University) for assistance in editing the language of a draft of this manuscript.

Funding

This study was funded by the Shanghai Science and Technology Commission (21Y11921800) and Zhongshan Hospital, Fudan University (2019ZSGG12 and 2020ZSLC24).

Conflict of interest

The authors have no conflict of interests related to this publication.

Author contributions

Study conceptualization (YC, MJ, DL, HJ, XZ, HG), experiment conduction (YC, MJ, YM, DL, HJ, SC), data acquisition, analysis, and interpretation (YC, MJ, JR), manuscript writing (MJ, YC, JR, XZ), review of the manuscript (MJ, YC, DL, HJ, SC, HG), and revision of the manuscript (MJ, YM, XZ, HG). All authors contributed to the article, reviewed, and agreed on all versions of the article before submission, during revision, the final version accepted for publication, and any significant changes introduced at the proofing stage. All authors agree to take responsibility and are accountable for the contents of the article.

Ethical statement

The study was approved by the Research Ethics Committee of Zhongshan Hospital, Fudan University [Approval no. B2018-070(2)]; the Animal Care and Use Committee of Zhongshan Hospital, Fudan University (Approval No. 2020-006). Written informed consent was obtained from the patient for the publication of this article. All animals received human care.

Data sharing statement

All data generated or analyzed during this study are included in this published article, its supplementary information files, and in the Gene Expression Omnibus database (GSE171874; RNA-seq data).

References

[1] Hoofnagle JH, Björnsson ES. Drug-Induced Liver Injury - Types and Phenotypes. N Engl J Med 2019;381(3):264–273. doi:10.1056/NEJMra1816149, PMID:31314970.
[2] Low EXS, Zheng Q, Chan E, Lim SG. Drug induced liver injury: East versus West - a systematic review and meta-analysis. Clin Mol Hepatol 2020;26(2):142–154. doi:10.3350/cmh.2019.1003, PMID:31816676.
[3] EFSA Panel on Contaminants in the Food Chain (CONTAM). Scientific Opinion on Pyrrolizidine alkaloids in food and feed. EFSA J 2011;9(11):2406. doi:10.2903/j.efsa.2011.2406.
[4] Miyata T, Tajima H, Hirata M, Nakanuma SI, Makino I, Hayashi H, *et al*. Phosphodiesterase III inhibitor attenuates rat sinusoidal obstruction syndrome through inhibition of platelet aggregation in Disse's space. J Gastroenterol Hepatol 2018;33(4):950–957. doi:10.1111/jgh.14004, PMID:28960464.
[5] Hirata M, Tajima H, Miyashita T, Miyata T, Nakanuma S, Makino I, *et al*. Extravasated platelet aggregation in the livers of rats with drug-induced hepatic sinusoidal obstruction syndrome. Mol Med Rep 2017;15(5):3147–3152. doi:10.3892/mmr.2017.6407, PMID:28358421.
[6] Chen Y, Jiang HY, Li DP, Chen SN, Wang JY, Gao H. Preliminary study of the changes in blood system in pyrrolizidine alkaloid-related liver damage. Zhonghua Gan Zang Bing Za Zhi 2021;29(6):533–538. doi:10.3760/cma.j.cn501113-20200630-00356, PMID:34225427.
[7] Munoz SJ, Stravitz RT, Gabriel DA. Coagulopathy of acute liver failure. Clin Liver Dis 2009;13(1):95–107. doi:10.1016/j.cld.2008.10.001, PMID:19150314.
[8] Groeneveld D, Cline-Fedewa H, Baker KS, Williams KJ, Roth RA, Mittermeier K, *et al*. Von Willebrand factor delays liver repair after acetaminophen-induced acute liver injury in mice. J Hepatol 2020;72(1):146–155. doi:10.1016/j.jhep.2019.09.030, PMID:31606553.
[9] Petri A, Kim HJ, Xu Y, de Groot R, Li C, Vandenbulcke A, *et al*. Crystal structure and substrate-induced activation of ADAMTS13. Nat Commun 2019;10(1):3781. doi:10.1038/s41467-019-11474-5, PMID:31439947.
[10] Driever EG, Stravitz RT, Zhang J, Adelmeijer J, Durkalski V, Lee WM, *et al*. VWF/ADAMTS13 Imbalance, But Not Global Coagulation or Fibrinolysis, Is Associated With Outcome and Bleeding in Acute Liver Failure. Hepatology 2021;73(5):1882–1891. doi:10.1002/hep.31507, PMID:32767567.
[11] Takaya H, Namisaki T, Kitade M, Kaji K, Nakanishi K, Tsuji Y, *et al*. VWF/ADAMTS13 ratio as a potential biomarker for early detection of hepatocellular carcinoma. BMC Gastroenterol 2019;19(1):167. doi:10.1186/s12876-019-1082-1, PMID:31638892.
[12] DeLeve LD, Wang X, Kuhlenkamp JF, Kaplowitz N. Toxicity of azathioprine and monocrotaline in murine sinusoidal endothelial cells and hepatocytes: the role of glutathione and relevance to hepatic venoocclusive disease. Hepatology 1996;23(3):589–599. doi:10.1002/hep.510230326, PMID:8617441.
[13] Zhuge Y, Liu Y, Xie W, Zou X, Xu J, Wang J, *et al*. Expert consensus on the clinical management of pyrrolizidine alkaloid-induced hepatic sinusoidal obstruction syndrome. J Gastroenterol Hepatol 2019;34(4):634–642. doi:10.1111/jgh.14612, PMID:30669184.
[14] Gao H, Ruan JQ, Chen J, Li N, Ke CQ, Ye Y, *et al*. Blood pyrrole-protein adducts as a diagnostic and prognostic index in pyrrolizidine alkaloid-hepatic sinusoidal obstruction syndrome. Drug Des Devel Ther 2015;9:4861–4868. doi:10.2147/DDDT.S87858, PMID:26346783.
[15] Li DP, Chen YL, Jiang HY, Chen Y, Zeng XQ, Xu LL, *et al*. Phosphocreatine attenuates Gynura segetum-induced hepatocyte apoptosis via a SIRT3-SOD2-mitochondrial reactive oxygen species pathway. Drug Des Devel Ther 2019;13:2081–2096. doi:10.2147/DDDT.S203564, PMID:31417240.
[16] Lin G, Wang JY, Li N, Li M, Gao H, Ji Y, *et al*. Hepatic sinusoidal obstruction syndrome associated with consumption of Gynura segetum. J Hepatol 2011;54(4):666–673. doi:10.1016/j.jhep.2010.07.031, PMID:21146894.
[17] Chen S, Zhou Y, Chen Y, Gu J. fastp: an ultra-fast all-in-one FASTQ preprocessor. Bioinformatics 2018;34(17):i884–i890. doi:10.1093/bioinformatics/bty560, PMID:30423086.
[18] Kim D, Paggi JM, Park C, Bennett C, Salzberg SL. Graph-based genome alignment and genotyping with HISAT2 and HISAT-genotype. Nat Biotechnol 2019;37(8):907–915. doi:10.1038/s41587-019-0201-4, PMID:31375807.
[19] Anders S, Pyl PT, Huber W. HTSeq—a Python framework to work with high-throughput sequencing data. Bioinformatics 2015;31(2):166–169. doi:10.1093/bioinformatics/btu638, PMID:25260700.
[20] Love MI, Huber W, Anders S. Moderated estimation of fold change and dispersion for RNA-seq data with DESeq2. Genome Biol 2014;15(12):550. doi:10.1186/s13059-014-0550-8, PMID:25516281.
[21] Yu G, Wang LG, Han Y, He QY. clusterProfiler: an R package for comparing biological themes among gene clusters. OMICS 2012;16(5):284–287. doi:10.1089/omi.2011.0118, PMID:22455463.
[22] Szklarczyk D, Gable AL, Lyon D, Junge A, Wyder S, Huerta-Cepas J, *et al*. STRING v11: protein-protein association networks with increased coverage, supporting functional discovery in genome-wide experimental datasets. Nucleic Acids Res 2019;47(D1):D607–D613. doi:10.1093/nar/gky1131, PMID:30476243.
[23] Yue C, Su J, Fan X, Song L, Jiang W, Xia J, *et al*. Immune-mediated thrombotic thrombocytopenic purpura in patients with and without systemic lupus erythematosus: a retrospective study. Orphanet J Rare Dis 2020;15(1):225. doi:10.1186/s13023-020-01510-9, PMID:32859237.
[24] Jurk K, Kehrel BE. Platelets: physiology and biochemistry. Semin Thromb Hemost 2005;31(4):381–392. doi:10.1055/s-2005-916671, PMID:16149014.
[25] Libersan D, Khalil A, Dagenais P, Quan E, Delorme F, Uzan A, *et al*. The low molecular weight heparin, enoxaparin, limits infarct size at reperfusion in the dog. Cardiovasc Res 1998;37(3):656–666. doi:10.1016/s0008-6363(97)00292-7, PMID:9659449.

[26] Zhao J, Falotico R, Nguyen T, Cheng Y, Parker T, Davé V, *et al*. A nonelutable low-molecular weight heparin stent coating for improved thromboresistance. J Biomed Mater Res B Appl Biomater 2012;100(5):1274–1282. doi:10.1002/jbm.b.32692, PMID:22454106.
[27] Xu XR, Zhang D, Oswald BE, Carrim N, Wang X, Hou Y, *et al*. Platelets are versatile cells: New discoveries in hemostasis, thrombosis, immune responses, tumor metastasis and beyond. Crit Rev Clin Lab Sci 2016;53(6):409–430. doi:10.1080/10408363.2016.1200008, PMID:27282765.
[28] Pradhan-Sundd T, Gudapati S, Kaminski TW, Ragni MV. Exploring the Complex Role of Coagulation Factor VIII in Chronic Liver Disease. Cell Mol Gastroenterol Hepatol 2021;12(3):1061–1072. doi:10.1016/j.jcmgh.2021.02.014, PMID:33705963.
[29] Sadler JE. Pathophysiology of thrombotic thrombocytopenic purpura. Blood 2017;130(10):1181–1188. doi:10.1182/blood-2017-04-636431, PMID:28768626.
[30] Balaphas A, Meyer J, Sadoul K, Fontana P, Morel P, Gonelle-Gispert C, *et al*. Platelets and Platelet-Derived Extracellular Vesicles in Liver Physiology and Disease. Hepatol Commun 2019;3(7):855–866. doi:10.1002/hep4.1358, PMID:31304449.
[31] Liang C, Takahashi K, Furuya K, Oda T, Ohkohchi N. Platelets Stimulate Liver Regeneration in a Rat Model of Partial Liver Transplantation. Liver Transpl 2021;27(5):719–734. doi:10.1002/lt.25962, PMID:33277780.
[32] Scheiner B, Kirstein M, Popp S, Hucke F, Bota S, Rohr-Udilova N, *et al*. Association of Platelet Count and Mean Platelet Volume with Overall Survival in Patients with Cirrhosis and Unresectable Hepatocellular Carcinoma. Liver Cancer 2019;8(3):203–217. doi:10.1159/000489833, PMID:31192156.
[33] Otaka F, Ito Y, Goto T, Eshima K, Amano H, Koizumi W, *et al*. Platelets prevent the development of monocrotaline-induced liver injury in mice. Toxicol Lett 2020;335:71–81. doi:10.1016/j.toxlet.2020.10.007, PMID:33122006.
[34] Scully M, Hibbard C, Ewenstein B. Recombinant ADAMTS 13 in thrombotic thrombocytopenic purpura. Oncoscience 2017;4(11-12):160–161. doi:10.18632/oncoscience.380, PMID:29344548.
[35] Scully M, Knöbl P, Kentouche K, Rice L, Windyga J, Schneppenheim R, *et al*. Recombinant ADAMTS-13: first-in-human pharmacokinetics and safety in congenital thrombotic thrombocytopenic purpura. Blood 2017;130(19):2055–2063. doi:10.1182/blood-2017-06-788026, PMID:28912376.
[36] Uemura M, Tatsumi K, Matsumoto M, Fujimoto M, Matsuyama T, Ishikawa M, *et al*. Localization of ADAMTS13 to the stellate cells of human liver. Blood 2005;106(3):922–924. doi:10.1182/blood-2005-01-0152, PMID:15855280.
[37] Turner NA, Nolasco L, Ruggeri ZM, Moake JL. Endothelial cell ADAMTS-13 and VWF: production, release, and VWF string cleavage. Blood 2009;114(24):5102–5111. doi:10.1182/blood-2009-07-231597, PMID:19822897.